

Experimental and Theoretical Studies of Laser-Generated Sulfur Polycarbon Hydride Ions: Collision-Induced Dissociation and *ab Initio* Calculations

Zhao-yang Liu, Zi-chao Tang, Rong-bin Huang, Qiang Zhang, and Lan-sun Zheng*

State Key Laboratory for Physical Chemistry of Solid Surface, Department of Chemistry, Xiamen University, Xiamen 361005, China

Received: January 8, 1997; In Final Form: March 25, 1997[⊗]

Both sulfur polycarbon hydride cations and anions were generated by laser ablating the mixture of carbon and sulfur powders and were further investigated experimentally and theoretically by means of collision-induced dissociation and *ab initio* calculations respectively. The computation results agree very well with the mass spectrometric results in the stability and connectivity of these species. Both experimental and theoretical results illustrate that the connectivity of the cluster ions is H–C–····–C–S, their stability alternates with the number of the clustering carbon atoms, and C–S is the weakest bond in all species. The results also reveal the opposite parity of the alternation effect between the positive and negative cluster ions: HC_{*n*}S⁺ with odd *n* is more stable, while HC_{*n*}S[−] with even *n* is more stable.

I. Introduction

Since the discovery¹ and successful preparation of C₆₀,² carbon clusters, especially with larger size, e.g., fullerenes, have become one of the most highlighted scientific research fields of the last decade.^{3,4} Meanwhile, smaller-sized carbon clusters with linear configuration have been of interest for many years both experimentally and theoretically.^{5,6} Such an interest is due to the involvement of these species in the chemistry of the interstellar medium, where reactivity is forfeited by quasi-collisionless conditions. Under these conditions, carbon takes the highly stable, albeit highly reactive, form of linear chains; some of the chains may be terminated by hydrogen atoms or by heteroatoms such as nitrogen, oxygen, or silicon.⁷ Addition of heteroatoms or groups presents a variety of stability to carbon chain. For example, carbon suboxide, C₃O₂, is a stable compound under ordinary conditions,⁸ C_{*n*}N₂ was synthesized by means of arc discharge,⁹ and carbon chains with as many as 20 atoms, stabilized by a group on two ends, have also been prepared.¹⁰ In gas phase, carbon cluster anions containing a heteroatom, C_{*n*}X[−] (X = B, Al, N, P, As, Bi, and *et al.*) were produced by laser ablating the proper samples.¹¹ Their abundance exhibits odd/even alternation, which varied with the number of clustering carbon atoms and the nature of the heteroatom.¹¹

The polycarbon sulfides C_{*n*}S and their protonated forms are also of interest to interstellar cloud chemistry.^{12,13} We have generated sulfur polycarbon hydride ions by laser ablating the mixture of sulfur and carbon powder.¹⁴ Like C_{*n*}X[−], an odd/even alternation in signal intensities was observed, and the cluster cations with even size and the anions with odd size were absent in the recorded mass spectra.¹⁴ R. Flammang *et al.*¹⁵ also observed C_{*n*}S⁺ and their hydrides in the electron impact mass spectrum of benzothiazole. In this paper, we report further mass spectrometry studies on the sulfur polycarbon hydrides ion by collision-induced dissociation on a homemade apparatus. Characterization of the species is verified by *ab initio* calculations.

II. Experimental Section

The crossed beam tandem time-of-flight mass spectrometer (TOFMS) employed in the experiments has been described in

detail previously,¹⁶ and only a brief description will be given here. The sulfur polycarbon hydride ions, generated by laser ablating the mixture of sulfur and carbon powders, diffused into the first acceleration region with their initial kinetic energy and then were accelerated by a pulsed field with a potential of 950 V. After flying through a 2.5 m field-free drift tube, ions with different masses were separated; then a kind of specific ion was selected by a pulsed field (the “mass gate”), and they were decelerated to 50–200 eV in kinetic energy. At the entry of the second acceleration region, the mass-selected ions collide with a crossed supersonic molecular beam. Both parent and daughter ions after the collision were accelerated by the second pulsed field with a total potential of 4000 V and analyzed by the second TOFMS with a 1.5 m field-free drift tube. To improve the signal to noise ratio of the recorded data, the pulsed gas valve was turned on and off alternatively, and the CID mass spectra were the difference between the ion signal detected with and without the colliding gas. In these spectra, the parent ion is shown as a negative-going peak, indicating its depletion by CID, and the fragment ions are shown as positive-going peaks.

The second harmonic output of a Quantary Nd:YAG laser, with wavelength 532 nm and pulse width 7 ns, was used. The power density irradiating on the sample surface was on the order of 10⁸ W cm^{−2} after being gently focused by an 80 cm focal-length lens. The mass resolution of the first TOFMS exceeds 400 and about 100 for the second. During the experiment, the apparatus was running under a vacuum of 10^{−4} Pa. The back-pressure of the colliding gas, highly purified nitrogen, was 2–4 atoms. The samples, carbon and sulfur powders, which are of spectrometric purity, were pressed into the sample holder after being well mixed. It was found that different mixed ratio did not affect the mass distribution of the product ions significantly.

III. Computational Details

Standard *ab initio* molecular orbital calculations were carried out with the Gaussian 92 system of programs. To avoid undesirable spin contamination, spin-restricted wave functions were employed. For closed-shell species, geometries were optimized at the RHF/6-31G* level, while the open-shell clusters were treated using the ROHF/6-31G* level. For the linear sulfur polycarbon hydride ions, there are two possible connectivities, hydrogen and sulfur atoms locating at each terminal, HC_{*n*}S[±], or both atoms locating at the same terminal to form a group,

* Corresponding author.

⊗ Abstract published in *Advance ACS Abstracts*, May 1, 1997.

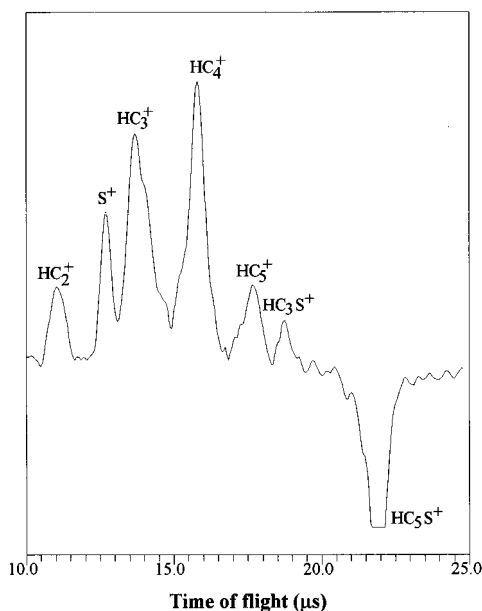
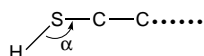


Figure 1. Collision-induced dissociation mass spectrum of HC_5S^+ . The mass spectrum was recorded by a difference technique. The mass-selected parent ion is shown as a negative-going peak, indicating its depletion by CID, and the fragment ions are indicated as positive-going peaks. Peaks of HC_5S^+ is off-scale.

HSC_n^\pm . The connectivity of SCH_n^\pm is chemically impossible. In addition to the bond lengths, the bond angle $\angle\text{HSC}$ of HSC_n^\pm may not be 180° , so it was also optimized in the computation:



In addition to the sulfur polycarbon hydride ions, another possible connectivity of the species is the type $\text{HC}_{n-m}\text{SC}_m^\pm$ ($m > 0$), in which the sulfur atom is inserted into the carbon chain. Though the structure is chemically possible, it is certainly unfavored in structural stability and not supported by the experimental observations. Besides, in the previous experimental and theoretical studies of C_nO ,^{25–28} C_nS^+ ,¹⁵ and HC_nS^+ ,¹⁵ the heteroatom was also found at the end of the carbon chain. So the structure was not considered in the calculations.

IV. Experimental Results

The sulfur polycarbon hydride ions were generated by laser ablation, and their mass distributions have already been described previously.¹⁴ Though the sample consisted of only sulfur and carbon, all polycarbon sulfide ions generated in the experiments were protonated. The hydrogen atom may come from the contaminant in the high-vacuum system, suggesting that the polycarbon sulfide ions must have strong affinity to the hydrogen atom so as to have their all valence electrons paired. It has been noticed that no sulfur polycarbon hydride cations with an even number of carbon atoms and no anions with an odd number of carbon atoms were observed. The similar effect, dependence of the parity on the charge of cluster ions, was also observed in C_nN^\pm , in which only C_nN^+ ¹⁷ with even n and C_nN^- with odd n ¹⁸ were detected. Therefore, only cations with an odd number of carbon atom and anions with an even number were investigated in the CID experiment reported in this paper.

Figure 1 is a typical CID mass spectrum shown as an example. The instrumental parameters were carefully adjusted during the experiments so that the areas of the positive-going and negative-going peaks are approximately equal. The CID results of sulfur polycarbon hydride cations and anions were summed in Tables 1 and 2 respectively; only the data for HC_nS^+

TABLE 1: Fragment Ions Produced from the Collision-Induced Dissociation of HC_nS^+ with Odd n ($n = 3–13$)^a

parent ions	fragment ions and their relative abundance							
HC_3S^+	HC_3^+ (43)	CS^+ (28)	S^+ (23)	HC_2^+ (6)				
HC_5S^+	HC_4^+ (26)	HC_3^- (25)	S^+ (14)	HC_2^+ (13)	C^+ (13)	HC_3S^+ (6)	C_5^+ (3)	
HC_7S^+	HC_6^+ (30)	C_3^+ (24)	HC_4^+ (13)	HC_5^+ (10)	CS^+ (8)	S^+ (6)	C_2^+ (6)	HC_7^+ (3)
HC_9S^+	HC_5^+ (29)	HC_3^+ (24)	C_4^+ (14)	HC_8^+ (9)	C_2^+ (9)	C^+ (8)	CS^+ (7)	
HC_{11}S^+	HC_7^+ (33)	HC_{10}^+ (27)	HC_5^+ (15)	C_3^+ (10)	CS^+ (10)	C_{11}^+ (5)		
HC_{13}S^+	HC_9^+ (35)	HC_{12}^+ (29)	C_7^+ (18)	HC_3S^+ (8)	C_5^+ (7)	C_8^+ (3)		

^a The relative abundance of each daughter ion is presented as a percentage of the depleted parent ion. Losing a sulfur atom (for ions of smaller size) or a CS group (for larger size) is the main dissociation channel.

with odd n and HC_nS^- with even n are listed. In the tables, the relative abundance of each daughter ions is presented as a percentage of the depleted parent ion. The fragmentation branching ratios were estimated from integration of the daughter ions' peaks in the recorded dissociation mass spectra. The estimated error is less than 5%. Though the parity of the positive and negative cluster ions is opposite, odd for cations and even for anions, their dissociation patterns are very similar. Losing a sulfur atom (for ions of smaller size) or a CS group (for larger size) is their main dissociation channel.

Under our experimental conditions, multistep collision and fragmentation are plausible. In fact, products from multistep fragmentation were also observed, especially for the parent ions with larger size. From the fragments shown in the tables, the daughter ions, $\text{C}_{n-1}\text{H}^\pm$, could lose a C_3 unit subsequently as the bare carbon cluster ions,^{19–22} but no fragment ions resulting from ejecting H were observed.

V. Theoretical Results

The total energies (E_n) obtained for HC_nS^\pm and HSC_n^\pm ($n = 1–9$) at the RHF/6-31G* level (note: ROHF for open-shell species) are presented in Tables 3 and 4 respectively. The energies were calculated from the optimized lowest energy geometry. The ground state of the cluster ions depends on the parity and connectivity of the species and is shown as follows:

¹ Σ : HC_nS^+ ($n = \text{odd number}$) and HC_nS^- ($n = \text{even number}$)

³ Σ : HC_nS^+ ($n = \text{even number}$) and HC_nS^- ($n = \text{odd number}$)

¹ A'' : HSC_n^+ ($n = \text{odd number}$) and HSC_n^- ($n = \text{even number}$)

³ A'' : HSC_n^+ ($n = \text{even number}$) and HSC_n^- ($n = \text{odd number}$)

Similar results have been found in C_nN^+ .¹⁷ For the cluster ions with the same clustering carbon atoms, the total energy of HC_nS^\pm is lower than that of its isomer, HSC_n^+ . The calculated energy different between adjacent clusters (ΔE), average binding energies (E_b), binding energy of the carbon atom (E_c), vertical ionization potential (VIP), and vertical electronic affinity (VEA) are also listed in Tables 3 and 4. E_b is obtained in the way described in ref 23, and E_c is defined as

$$E_c = E(\text{HC}_n\text{S}^\pm) - E(\text{HC}_{n-1}\text{S}^\pm) - E(\text{C})$$

As shown in the tables, values of E_b , E_c , VIP, and VEA exhibit the odd/even alternation as well.

The optimized geometric parameters for the lowest energy state of the two structural isomers, HC_nS^\pm and HSC_n^+ ($n = 1–9$), are illustrated in Figures 2 and 3, respectively. In addition to the data of bond lengths, data for the bond angle $\angle\text{HSC}$ of HSC_n^+ is presented just below the bond lengths. Examining

TABLE 2: Fragment Ions Produced from the Collision-Induced Dissociation of HC_nS^- with Even n ($n = 4-18$)^a

parent ions	fragment ions and their relative abundance									
HC_4S^-	HC_4^- (41)	C_3^- (22)	C_4^- (20)	HC^- (12)	S^- (5)					
HC_6S^-	HC_6^- (54)	HC_5^- (35)	C_4^- (11)							
HC_{10}S^-	HC_9^- (23)	HC_6^- (19)	C_4^- (15)	C_5^- (12)	HC_{10}^- (9)	HC_8^- (9)	C_7^- (8)	HC^- (3)	S^- (2)	
HC_{12}S^-	HC_{11}^- (26)	HC_{12}^- (22)	HC_8^- (16)	C_3S^- (11)	C_2S^- (8)	HC_6S^- (8)	HC_{10}S^- (4)	HC_{10}^- (3)	S^- (2)	
HC_{14}S^-	HC_{10}^- (34)	HC_{13}^- (18)	HC_{14}^- (15)	C_4S^- (13)	HC_8^- (12)	HC_9^- (8)				
HC_{16}S^-	HC_{12}^- (29)	C_5S^- (23)	HC_5^- (18)	HC_6^- (16)	HC_{15}^- (14)					
HC_{18}S^-	HC_{14}^- (22)	HC_{17}^- (19)	HC_{13}^- (15)	HC_{12}^- (13)	HC_{10}^- (9)	HC_{11}^- (7)	C_8^- (6)	C_5S^- (5)	HC_{12}S^- (4)	

^a As in the cations, the relative abundance of each daughter ion is presented as a percentage of the depleted parent ion. Losing a sulfur atom (for ions of smaller size) or a CS group (for larger size) is the main dissociation channel.

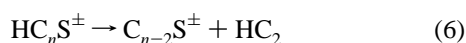
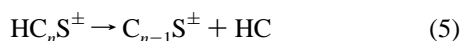
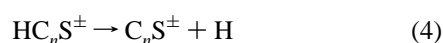
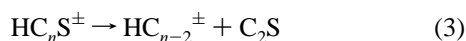
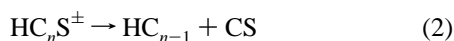
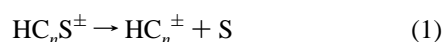
TABLE 3: The Total Energies (E_n), the Energy Difference between Neighboring Clusters (ΔE) (in au), the Average Binding Energies (E_b), the Binding Energies of Carbon Atoms (E_c) of HC_nS^+ and HSC_n^+ , and the Vertical Ionization Potential (in eV) of HC_nS and HSC_n ^a

species	HCS^+	HC_2S^+	HC_3S^+	HC_4S^+	HC_5S^+	HC_6S^+	HC_7S^+	HC_8S^+	HC_9S^+
E_n	-435.610	-473.416	-511.312	-549.116	-587.002	-624.806	-662.686	-700.490	-738.369
ΔE_n		-37.806	-37.896	-37.804	-37.886	-37.804	-37.880	-37.804	-37.879
E_b	1.007	1.252	2.830	2.966	3.537	3.510	3.809	3.755	3.945
E_c		-5.630	-8.078	-5.576	-7.806	-5.576	-7.643	-5.576	-7.616
VIP	6.775	6.639	6.558	6.608	6.395	5.633	6.340	6.496	6.258
species	HSC^+	HSC_2^+	HSC_3^+	HSC_4^+	HSC_5^+	HSC_6^+	HSC_7^+	HSC_8^+	HSC_9^+
E_n	-435.496	-473.316	-511.195	-549.016	-586.886	-624.706	-662.571	-700.392	-738.253
ΔE_n		-37.820	-37.879	-37.821	-37.870	-37.820	-37.865	-37.821	-37.861
E_b	-4.109	-0.109	1.769	2.313	2.884	3.048	3.347	3.429	3.592
E_c		-6.011	-7.616	-6.038	-7.371	-6.011	-7.235	-6.038	-7.126
VIP	8.980	9.551	7.918	8.843	7.537	10.041	7.374	8.218	7.292

^a All calculations were carried out at the RHF/6-31G* level for odd n species and the ROHF/6-31G* level for even species.

the geometric data shown in the figures, it can be found that the C-S bond length of HC_nS^- is longer than that of HC_nS^+ , and the latter alternates between the cations with even and odd n . Besides, the length of the H-C bond in HC_nS^- is slightly shorter than that of HC_nS^+ . The C-C bond length of the cluster ions also exhibits alternative behavior: for HC_nS^+ with odd n and HC_nS^- with even n , the bond length of C-C alternates regularly, implying a polyacetylenic bonding structure. But for HC_nS^+ with even n and HC_nS^- with odd n , the C-C bonds near the terminal sulfur atom tend to be equalized so as to exhibit the cumulative double-bonding character.

As part of the theoretical studies, the dissociation energy of the cluster ions has been calculated. Since HC_nS^\pm is more stable than its isomer, HSC_n^\pm , only the dissociation channel and corresponding dissociation energy of the former are considered. In this configuration, the two heteroatoms, H and S, locate at two ends of the carbon chain, so its possible dissociation channels are more complicated. For the work reported in this paper, we calculated the dissociation energies of following dissociation channels:



The calculated dissociation energies are plotted in Figures 4 and 5 respectively, as the functions of the number of the clustering carbon atoms. Like the CID experimental results described above, the calculated results of the cluster cation and anions shown in the two figures look very similar. For example, except the fragmentation energy of losing C_2S , which decreases with increase of cluster size, the fragmentation energy of each dissociation channel alternates with the parity of the clustering carbon atoms. Fragmentation energies of relatively unstable species, HC_nS^+ with even n and HC_nS^- with odd n , are less than those of their neighbors. For those relatively stable species which were observed and investigated in the mass spectrometry, ejection of the sulfur atom is the lowest energy dissociation path for both positive and negative ions.

To examine the effect of correlation and basis set size, smaller clusters with number of carbon atoms less than five were calculated at the CI/6-311*G level. The result shows the same even/odd alternation tendency and confirms that the HC_nS^\pm connectivity is more stable. Hence, RHF or ROHF/6-31*G is an acceptable choice for computing the clusters with carbon numbers as large as nine.

VI. Discussion

1. Connectivity of HC_nS^\pm . As mentioned above, even though carbon clusters larger than 6 in size, especially with even size, may take plane-cyclic configuration, all carbon clusters with a heretoatom, C_nN ,¹⁷ C_nN^- ,^{18,24} C_nO ,²⁵⁻²⁸ C_nP^- ,²⁹ *et al.*, have a linear configuration with size up to 11. However, there are two heteroatoms in sulfur polycarbon hydride ions. If the heteroatoms locate at the ends of the carbon chain, they can have two possible isomers: $[\text{H}-\text{C}_n\text{S}]^\pm$ or $[\text{C}_n-\text{S}-\text{H}]^\pm$, except

TABLE 4: The Total Energies (E_n) the Energy Difference between Adjacent Clusters (ΔE) (in au), the Average Binding Energies (E_b) the Binding Energies of Carbon Atoms (E_c) of HC_nS^- and HSC_n^- , and the Vertical Electron Affinities (in eV) of HC_nS^- and HSC_n^-

species	HCS^-	HC_2S^-	HC_3S^-	HC_4S^-	HC_5S^-	HC_6S^-	HC_7S^-	HC_8S^-	HC_9S^-
E_n	-435.843	-473.785	-511.565	-549.483	-587.268	-625.174	-662.962	-700.860	-738.650
ΔE_n		-37.942	-37.780	-37.918	-37.785	-37.906	-37.788	-37.898	-37.790
E_b	5.333	6.286	5.116	5.469	4.980	5.170	4.871	5.007	4.789
E_c		-9.330	-4.923	-8.677	-5.059	-8.350	-5.141	-8.133	-5.195
VEA	0.435	-1.687	-0.327	-1.878	-0.844	-2.150	-1.171	-2.286	-1.388

species	HSC^-	HSC_2^-	HSC_3^-	HSC_4^-	HSC_5^-	HSC_6^-	HSC_7^-	HSC_8^-	HSC_9^-
E_n	-435.809	-473.704	-511.492	-549.402	-587.194	-625.094	-662.885	700.781	-738.572
ΔE_n		-37.895	-37.788	-37.910	-37.792	-37.900	-37.791	-37.896	-37.791
E_b	4.408	5.170	4.463	4.925	4.571	4.816	4.571	4.735	4.544
E_c		-8.051	-5.141	-8.459	-5.250	-8.187	-5.222	-8.078	-5.222
VEA	0.463	-1.007	-0.163	-1.660	-0.844	-2.694	-1.116	-2.367	-1.388

^a All the calculation were carried out at the RHF/6-31G* level for even n species and the ROHF/6-31G* level for odd species.

H 1.0739 C 1.4542 S	H 1.0584 C 1.6932 S
H 1.0676 C 1.2909 C 1.5022 S	H 1.0548 C 1.2024 C 1.6948 S
H 1.0654 C 1.1950 C 1.3491 C 1.4739 S	H 1.0534 C 1.2217 C 1.3214 C 1.6504 S
H 1.0643 C 1.2007 C 1.3331 C 1.2684 C 1.5242 S	H 1.0548 C 1.1966 C 1.3771 C 1.2092 C 1.6692 S
H 1.0626 C 1.1916 C 1.3609 C 1.2063 C 1.3339 C 1.4826 S	H 1.0542 C 1.2072 C 1.3427 C 1.2903 C 1.2449 C 1.6492 S
H 1.0622 C 1.1928 C 1.3581 C 1.2157 C 1.3130 C 1.2745 C 1.5228 S	H 1.0553 C 1.1932 C 1.3798 C 1.2033 C 1.3636 C 1.2132 C 1.6570 S
H 1.0610 C 1.1899 C 1.3690 C 1.2007 C 1.3487 C 1.2110 C 1.3277 C 1.4870 S	H 1.0551 C 1.1962 C 1.3714 C 1.2200 C 1.3213 C 1.2919 C 1.2448 C 1.6313 S
H 1.0608 C 1.1901 C 1.3684 C 1.2027 C 1.3437 C 1.2226 C 1.3048 C 1.2758 C 1.5237 S	H 1.0557 C 1.1912 C 1.3819 C 1.1991 C 1.3690 C 1.2065 C 1.3574 C 1.2154 C 1.6502 S
H 1.0599 C 1.1887 C 1.3746 C 1.1970 C 1.3595 C 1.2039 C 1.3442 C 1.2133 C 1.3246 C 1.4891 S	H 1.0556 C 1.1924 C 1.3793 C 1.2037 C 1.3508 C 1.2266 C 1.3115 C 1.2927 C 1.2448 C 1.6251 S
(a)	(a)
H 1.3502 S 1.6093 C 88.296	H 1.3371 S 1.2007 C 101.311
H 1.3351 S 1.6336 C 1.3335 C 95.142	H 1.3351 S 1.6336 C 1.3335 C 95.142
H 1.3328 S 1.6376 C 1.2311 C 1.3181 C 94.890	H 1.3370 S 1.6819 C 1.2200 C 1.4128 C 101.358
H 1.3309 S 1.6430 C 1.2285 C 1.3141 C 1.3106 C 95.707	H 1.3309 S 1.6430 C 1.2285 C 1.3141 C 1.3106 C 95.707
H 1.3296 S 1.6567 C 1.2146 C 1.3211 C 1.2374 C 1.3096 C 95.630	H 1.3317 S 1.6959 C 1.2043 C 1.3605 C 1.2352 C 1.3555 C 100.026
H 1.3294 S 1.6513 C 1.2192 C 1.3231 C 1.2328 C 1.3136 C 1.3005 C 96.182	H 1.3294 S 1.6513 C 1.2192 C 1.3231 C 1.2328 C 1.3136 C 1.3005 C 96.182
H 1.3282 S 1.6705 C 1.2068 C 1.3385 C 1.2189 C 1.3146 C 1.2407 C 1.3051 C 95.900	H 1.3294 S 1.6982 C 1.1984 C 1.3705 C 1.2122 C 1.3451 C 1.2436 C 1.3051 C 98.991
H 1.3286 S 1.6568 C 1.2151 C 1.3288 C 1.2266 C 1.3222 C 1.2276 C 1.3213 C 1.2915 C 96.560	H 1.3286 S 1.6568 C 1.2151 C 1.3288 C 1.2266 C 1.3222 C 1.2276 C 1.3213 C 1.2915 C 96.560
H 1.3274 S 1.6814 C 1.2029 C 1.3562 C 1.2092 C 1.3342 C 1.2206 C 1.3132 C 1.2422 C 1.3029 C 96.017	H 1.3283 S 1.6991 C 1.1955 C 1.3757 C 1.2038 C 1.3598 C 1.2167 C 1.3363 C 1.2504 C 1.3237 C 98.309
(b)	(b)

Figure 2. Optimized geometric parameter of two isomers of sulfur polycarbon hydride cations: (a) linear HC_nS^+ and (b) bent HC_nS^+ at the RHF/6-31G* level (ROHF for open-shell species). The electronic state of odd n HC_nS^+ and HSC_n^+ is $^1\Sigma$ and $^1A''$, respectively, and that of corresponding even species is $^1\Sigma$ and $^3A''$. The bond angles $\angle\text{HSC}$ in HSC_n^+ are listed just below their bond lengths. The bond lengths are in angstroms and angles in degrees.

for $[\text{S}-\text{H}-\text{C}_n]^{\pm}$ which is chemically impossible. From the calculated total energies listed in Tables 3 and 4, between the pair of the structural isomers, the former is more stable. Therefore, if the sulfur polycarbon hydride ions produced from laser ablation and observed in the recorded mass spectra are thermodynamically favored, their connectivity should be the former. The suggestion is supported by the results of CID experiments.

In the experiments, the positive and negative cluster ions were produced from direct laser vaporization. Since buffer gas was

Figure 3. Optimized geometric parameter of two isomers of sulfur polycarbon hydride anions: (a) linear HC_nS^- and (b) bent HC_nS^- at the RHF/6-31G* level (ROHF for open-shell species). The electronic state of odd n HC_nS^- and HSC_n^- is $^1\Sigma$ and $^1A''$, respectively, and that of corresponding even species is $^3\Sigma$ and $^3A''$. The bond angles $\angle\text{HSC}$ in HSC_n^- are listed just below their bond lengths. The bond lengths are in angstroms and angles in degrees.

not introduced in the experiments, the ions must be well excited. However, there is about a 100–200 μs delay between the vaporization laser pulse and the ion extraction pulse, so most observed ions may have enough time to give off their extra internal energy from radiation and radiationless transition. The observation that less stable clusters (cations with an even number of carbon atoms and anions with odd carbons) were almost not detected in the experiments suggests that the detected ions were actually not very hot. According to the calculations, the difference in stability between odd and even clusters is about

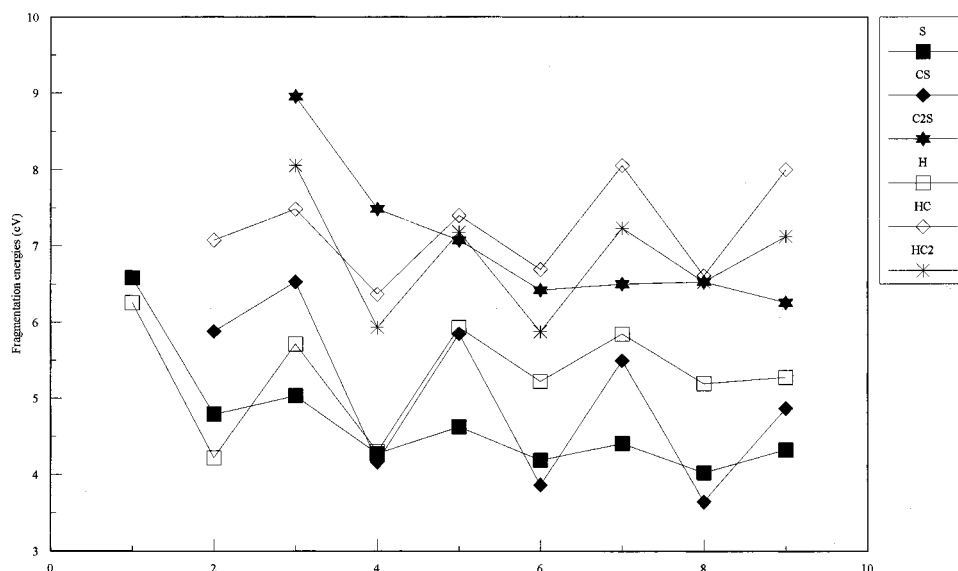


Figure 4. Calculated fragmentation energies (in eV) of linear HC_nS^+ by losing S, CS, C_2S , H, HS, and HSC unit versus the number of clustering carbon atoms. All calculations were carried out at the RHF/6-31G* level for odd n species and the ROHF/6-31G* level for even species.

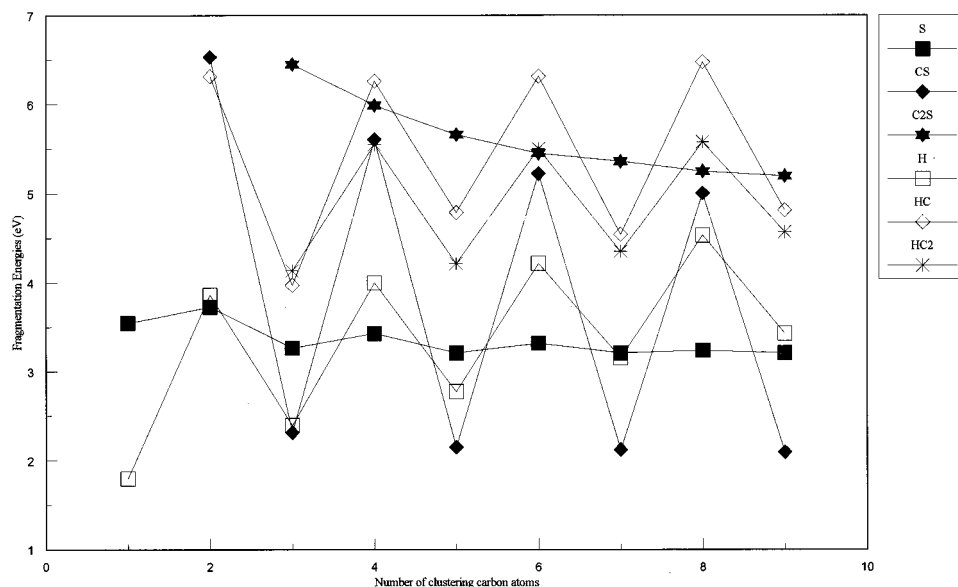


Figure 5. Calculated fragmentation energies (in eV) of linear HC_nS^- by losing S, CS, C_2S , H, HS, and HSC unit versus the number of clustering carbon atoms. All calculations were carried out at the RHF/6-31G* level for even n species and the ROHF/6-31G* level for odd n species.

1.6 eV. From the energy difference, we can estimate that the temperature of the observed cluster ions is less than 2000 K, supposing that the relative abundance of the less stable clusters is less than 1%. Therefore, though the cluster ions were generated in high-temperature plasma, they cannot be excited well above the barrier to isomerization, and the CID results are useful to interpret the structures of the clusters.

Inspecting the fragment ions shown in Tables 1 and 2, one can easily notice that the predominant fragments are HC_m^+ ($m \leq n$), and almost no C_n^\pm or SH^\pm is observed. Since the connectivity, $\text{C}-\cdots-\text{C}-\text{H}-\text{S}$, is chemically impossible, the two heteroatoms, H and S, must locate at each end of the carbon chain. With the increase of the cluster size, fragment ions HC_mS^\pm ($m < n$) produced from losing a certain number of carbon atoms could be detected, suggesting that both structural isomers may coexist. As a matter of fact, losses of atoms from internal positions of the linear species have been noticed in the collisional activation (CA) and neutralization-reionization (NR) studies of silicon polycarbon hydrides SiC_nH ($n = 4, 6$) and were attributed to multicenter processes.³⁰ During the reactions, the linear species may be in a cyclic transition state to form their isomers, as long as their sizes are large enough to reduce

the tension in the rearrangement. Hence, ejection of carbon atoms or clusters from the sulfur polycarbon hydride ions of larger sizes may follow the isomeric reactions, and the connectivity of most cluster ions produced in the experiment can be described as $\text{H}-\text{C}-\cdots-\text{C}-\text{S}$.

2. The Stability of HC_nS^\pm . In our experimental conditions, only HC_nS^+ with even n and HC_nS^- with odd n could be observed.¹⁴ The mass distribution suggests that HC_nS^+ with odd n and HC_nS^- with even n are unstable. Our calculated results agree with the experimental observation.

The total energy of a molecule is the most important criterion for its stability, but it is only good for comparison of its structural isomers. To compare the relative stability of the clusters with different sizes, energy difference between the adjacent clusters, $\Delta E_n = E_n - E_{n-1}$, is more informative. Meanwhile, the average binding energy (E_b), the binding energy of carbon atom (E_c), vertical ionization energy (VIP), and/or vertical electronic affinity (VEA) are also the important parameters to evaluate their relative stability. Table 3 lists the ΔE_n , E_b , VIP, and VEA of HC_nS^\pm . These relative values exhibit a dramatic even/odd alternation, in good agreement with the observed mass distribution. According to the calculated values,

ΔE_n of HC_nS^+ with odd n is lower than that of even-numbered ones, indicating that the former is more stable. The same analysis and conclusion can also be applied to the anions, suggesting that even-numbered HC_nS^- is more stable. The definition of E_b implies that the larger the E_b of the species is, the more stable it is. Inspecting the values of E_b listed in the table, the same conclusion can be reached that HC_nS^+ with odd n and HC_nS^- with even n are more stable. The calculated values of VIP and VEA are also consistent with the conclusion.

The even/odd alternation of the structural stability can also be characterized from the optimized bond lengths of the sulfur polycarbon hydride ions. For the positive ions, the C–S bond of the odd-numbered ions is shorter than that of the even-numbered ones, so the former is more stable. The C–S bond of the negative ions is a single bond and does not show such alternation effect, but the effect can be perceived from C–C bond lengths of the anions. The C–C bond of the even-numbered ions is polyacetylene-like with triple–single bond alternation, but in the odd-numbered species, the bonds near the sulfur atom are cumulen-like. Obviously, structure of the former is thermodynamically favored.

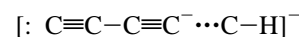
In the laser ablation experiment, both positive and negative ions of the sulfur polycarbon hydrides can be generated and recorded at the same time. They have same structure and composition. Their only difference is the two electrons resulting from the opposite charge carried by the single-charged species. It is interesting to note that the difference can invert the parity of the alternation effect. According to the molecular orbital calculation, the HOMO of the sulfur polycarbon hydride ions is the doubly degenerated π orbital. For HC_nS^+ with odd n , the orbital is fully filled; it therefore has a stable electronic structure. The ground state of the cation with an even number of carbons, however, is the triplet state, so its HOMO is only half-filled. With the additional two electrons, the doubly degenerated HOMO of HC_nS^- with even n will become half-filled and that of the anions with even size is fully filled, so the latter is more stable.

3. Dissociation Channels and Fragmentation Energies of HC_nS^\pm . In addition to exhibiting the alternation effect, comparing with the calculated fragmentation energy of different dissociation channels helps to characterize the structure of the cluster ions. In Figures 4 and 5, the fragmentation energies are displayed as functions of the number of clustering carbon atoms. As shown in the figures, for HC_nS^+ with odd n and HC_nS^- with even n , ejection of the sulfur atom is the lowest-energy dissociation pathway, but for even HC_nS^+ and odd HC_nS^- , the weakest bond is the C–C bond next to the sulfur atom. Some dissociation channels, such as the ejection of S or C_2S , do not change the parity of the parent ions, so the alternation effect may not be very significant, but if the lost fragment contains single carbon atom (CS or CH), the parity of the daughter ions will be inverted, so that the effect shown in the figures is very dramatic.

The results from CID experiment are in good agreement with the *ab initio* calculations. In the experiment, the studies can reach the cluster ions with larger sizes, so other dissociation pathways can also be distinguished. For HC_nS^\pm with relatively small sizes, the predominant daughter ion is HC_{n-1}^\pm from losing the single sulfur atom. As the length of the carbon chain increases, the daughter ion, HC_{n-1}^\pm , was also observed and gradually becomes the main fragment. In our experimental conditions, multistep fragmentation can also take place, so the granddaughter or even great-granddaughter ions can also be observed. In fact, the daughter ions HC_{n-1}^\pm can further lose C_3 to be HC_{n-4}^\pm , like the bare carbon cluster ions, whose dissociation process has been well studied.^{19–22} For the cluster

ions with larger sizes, the granddaughter ion, HC_{n-4}^\pm , becomes the major fragment as shown in the tables.

In the experiments, only cations with an odd number of carbons and anions with even numbers could be produced and selected for the CID studies. However, the same dissociation channels have been observed for both positive and negative ions. The difference is the size effect to the dissociation channels. For example, among the fragment ions of HC_5S^+ , C_4H^+ is predominant, and C_5H^+ , which could be produced from ejection of S, is even not observed at all. But for the negative ions, loss of CS becomes the lowest-energy dissociation pathway only when the length of carbon chain is up to 10, and even for the cluster ions with such size, the daughter ions resulted from ejection of S can still be observed with considerable abundance. Similarly, observation of C_{n-4}H^+ as the predominant daughter cation appears at $n \geq 9$, but for the negative ions, the effect can be observed only at $n \geq 14$. The difference between the positive and negative ions can be correlated to the structural stability of the linear polycarbon hydride ions, C_nH^\pm . The valence bonding structure of C_nH^- with even n can be described as follows:



But the positive ions cannot have such stable polyacetylene structure, so they are easier to dissociate.

VII. Conclusion

Both positive and negative sulfur polycarbon hydride ions could be produced and were investigated by CID experiments. The species were also studied with *ab initio* calculations, assuming that the species are in linear configuration. The experimental and theoretical results agree very well in following aspects:

(1) Structural stability of both sulfur polycarbon hydride cations and anions exhibit a dramatic even/odd alternation effect, but the parity of the effect is opposite between the cation and anions. For the positive ions, those with an odd number of carbons are more stable, while the negative ions with an even number of carbons are more stable.

(2) For the sulfur polycarbon hydride ions in linear geometry, two structural isomers, HC_nS^\pm and HSC_n^\pm , are possible. The former is more stable.

(3) The lowest-energy dissociation pathway of the small sulfur polycarbon hydride ions is the ejection of the sulfur atom. As the length of the carbon chain increases, the C–C bond next to the sulfur atom becomes the weakest bond.

Acknowledgment. This work was supported by the Trans-century Training Program Foundation for Talents by the State Education Commission and the National Science Foundation of China.

References and Notes

- (1) Kroto, H. W.; Heath, J. R.; O'Brien, S. C.; Curl, R. F.; Smalley, R. E. *Nature* **1985**, *318*, 162.
- (2) Kratschmer, W.; Lamb, L. D.; Fostiropoulos, K.; Huffman, D. R. *Nature* **1990**, *347*, 354.
- (3) Taylor, R. *Interdiscip. Sci. Rev.* **1992**, *17*, 161.
- (4) Taylor, R.; Walton, D. R. M. *Nature* **1993**, *363*, 685.
- (5) Welter, W.; Van Zee, R. J. *Chem. Rev.* **1989**, *89*, 1713.
- (6) Hutter, J.; Luthi, H. P.; Diederich, F. *J. Am. Chem. Soc.* **1994**, *116*, 750.
- (7) Moazzen-Ahmadi, N.; Zerbetto, F. *J. Chem. Phys.* **1995**, *103*, 6343.
- (8) Kappe, T.; Ziegler, E. *Angew. Chem., Int., Ed. Engl.* **1974**, *13*, 491.
- (9) Grosser, T.; Hirsch, A. *Angew. Chem., Int. Ed. Engl.* **1993**, *32*, 1340.
- (10) Brady, M.; Weng, W. Q.; Gladysz, J. A. *J. Chem. Soc., Chem. Commun.* **1994**, 2655, 23.

- (11) Huang, R. B.; Wang, C. R.; Liu, Z. Y.; Qi, F.; Sheng, L. S.; Yu, S. Q.; Zheng, L. S. *Z. Phys. D.* **1995**, 33, 49.
- (12) Oshima, Y.; Endo, Y. *J. Mol. Spectrosc.* **1992**, 135, 627.
- (13) Hirahara, Y.; Oshima, Y.; Endo, Y. *Astrophys. J.* **1993**, L113, 408.
- (14) Liu, Z. Y.; Huang, R. B.; Zheng, L. S. *Int. J. Mass Spectrom. Ion Processes* **1996**, 155, 79.
- (15) Flammang, R.; Van Haverbeke, Y.; Wong, M. W.; Wentrup, C. *Rapid Commun. Mass Spectrom.* **1995**, 9, 208.
- (16) Huang, R. B.; Liu, Z. Y.; Liu, H. F.; Chen, L. H.; Zheng, Q.; Wang, C. R.; Zheng, L. S.; Liu, F. Y.; Yu, S. Q.; Ma, X. X. *Int. J. Mass Spectrom. Ion Processes* **1995**, 151, 55.
- (17) Resat, M. R.; Smolanoff, J. N.; Goldman, L. B. *J. Chem. Phys.* **1994**, 100, 8784.
- (18) Wang, C. R.; Huang, R. B.; Liu, Z. Y.; Zheng, L. S. *Chem. Phys. Lett.* **1995**, 237, 463.
- (19) Sowaresat, M. B.; Hintz, P. A.; Anderson, S. L. *J. Phys. Chem.* **1995**, 99, 10736.
- (20) Whetten, R. L.; Yerezian, C.; Stjohn, P. M. *Int. J. Mass Spectrom. Ion Processes* **1994**, 138, 63.
- (21) Hunter, J. M.; Fye, J. L.; Roskamp, E. J.; Jarrold, M. F. *J. Phys. Chem.* **1994**, 98, 1810.
- (22) Parent, D. C.; Anderson, S. L. *Chem. Rev.* **1992**, 92, 1541.
- (23) Bonacic-koutecky, V.; Fantucci, P.; Koutecky, J. *Chem. Rev.* **1991**, 91, 1035.
- (24) Botschwina, P. *Chem. Phys. Lett.* **1996**, 259, 627.
- (25) Maozzen-Ahmadi, N.; Zerbetto, F. *J. Chem. Phys.* **1995**, 103, 6343.
- (26) Gilliam, O. R.; Johson, C. M.; Gordy, W. *Phys. Rev.* **1950**, 78, 140.
- (27) Ohshima, Y.; Endo, Y.; Ogata, T. *J. Chem. Phys.* **1995**, 102, 1493.
- (28) Ogata, T.; Ohshima, Y.; Endo, Y. *J. Am. Chem. Soc.* **1995**, 117, 3593.
- (29) Liu, Z. Y.; Huang, R. B.; Zheng, L. S. Unpublished results.
- (30) Iraqi, N.; Schwarz, N. *Chem. Phys. Lett.* **1995**, 205, 183.